applied sciences

MDPI

Article

A QoS-Enabled Medium-Transparent MAC Protocol for Fiber-Wireless 5G RAN Transport Networks

George Kalfas [1,2,*], Dimitris Palianopoulos [1,2], Agapi Mesodiakaki [1,2], Marios Gatzianas [1,2], Christos Vagionas [1,2], Ronis Maximidis [1,2] and Nikos Pleros [1,2]

[1] Department of Informatics, Aristotle University of Thessaloniki, 54636 Thessaloniki, Greece
[2] Center for Interdisciplinary Research and Innovation, 57001 Thessaloniki, Greece
* Correspondence: gkalfas@csd.auth.gr

Abstract: In order to meet the ever-increasing 5G and beyond Radio Access Network (RAN) densification demands, Fiber-Wireless transport networks are expected to play a key role in accelerating 5G deployment by providing the essential RAN flexibility, while at the same time avoiding costly fiber-trenching. Due to the inefficiency of the Radio-and-Fiber (R&F) networks for application in dense RAN topologies, Analog-Radio-over-Fiber (A-RoF) technology is regarded as a key enabling solution, since it greatly simplifies the remote antenna while offering very high spectral efficiency. For this type of dense A-RoF network, new and efficient Medium-Transparent-Medium Access Control (MT-MAC) protocols are required that can concurrently arbitrate optical and wireless resources, while at the same time offering the necessary Quality-of-Service (QoS) for correct operation of the combined Fronthaul/Midhaul/Backhaul segments present in 5G disaggregated RANs. In this paper, we propose a QoS-enabled MT-MAC (qMT-MAC) protocol that can combine Fronthaul/Midhaul/Backhaul flows under the same framework, while satisfying the strict delay and jitter requirements set by the relevant standards. Results show that qMT-MAC concurrently achieves the delay and jitter requirements for combined Fronthaul/Midhaul/Backhaul traffic even when loads approach the network's capacity, while attested enhanced prioritization policies can offer up to a 64% delay reduction over State-of-the-Art MT-MAC protocols.

Keywords: analog Radio-over-Fiber (a-RoF) 5G; fronthaul; midhaul; backhaul; Disaggregated Radio Access Networks (D-RAN); Fiber-Wireless (FiWi); Medium-Transparent MAC (MT-MAC); Ultra-Reliable and Low-Latency Communications (URLLC); Quality-of-Service (QoS)

check for updates

Citation: Kalfas, G.; Palianopoulos, D.; Mesodiakaki, A.; Gatzianas, M.; Vagionas, C.; Maximidis, R.; Pleros, N. A QoS-Enabled Medium-Transparent MAC Protocol for Fiber-Wireless 5G RAN Transport Networks. *Appl. Sci.* **2022**, *12*, 8708. https://doi.org/10.3390/app12178708

Academic Editor: Peng-Chun Peng

Received: 29 June 2022
Accepted: 26 August 2022
Published: 30 August 2022

Publisher's Note: MDPI stays neutral with regard to jurisdictional claims in published maps and institutional affiliations.

Copyright: © 2022 by the authors. Licensee MDPI, Basel, Switzerland. This article is an open access article distributed under the terms and conditions of the Creative Commons Attribution (CC BY) license (https://creativecommons.org/licenses/by/4.0/).

1. Introduction

The global demand for mobile broadband capacity is increasing at an exponential rate, owing to the ever-expanding popularity of over-the-top streaming services [1], as well as the increase of Machine-to-Machine communications, which are expected to account for half of all globally connected devices by 2023 [1]. Adding to the above, forecasts for mobile traffic's annual growth of 4.8 zettabytes by 2023 [1] highlight the cause behind the Mobile Network Operators' (MNOs) desire for a swift and sustainable infrastructure update. To combat the demand surge, the New Radio (NR) Rel. 15 standard introduced a series of innovations, with one of them being the employment of the Millimeter Wave (mmWave) spectrum in the access network. The latter inherently offers a huge bandwidth for use in data communications and can, thus, greatly increase the mobile network capacity, providing a solution to the network congestion problem observed in densely populated areas. However, due to its inherently high path loss and gas/foliage attenuation losses, as well as enhanced reflection and scattering phenomena, mmWave carries a significantly shorter effective range compared to sub-6 GHz radio, thus necessitating the placement of the Access Points (APs) at close proximity to the user [2]. The above effectively pushes for intensive densification of the Radio Access Network (RAN), creating a two-fold problem:

(i) the interconnection of the numerous AP locations and (ii) the equipment expenditure associated with the acquisition and operation of the mmWave 5G NR APs. Regarding the first issue, fiber carries the advantage of immense capacity and, as such, has been established as the main sub-6 GHz RAN enabler. However, the RAN densification goals set by the mobile operators are being hampered by the high fiber trenching costs, as well as license fees to rights-of-way and regulatory requirements to access public or utility-owned sites [3]. All these immense costs lead to increased Capital Expenditures (CAPEX) and a longer Time-to-Market [4], prompting the industry to aggressively develop combined Fiber-Wireless (FiWi) RAN transport solutions to speed up 5G deployment and provide the essential RAN flexibility [5]. Regarding the second issue, 5G NR proposed RAN disaggregation, which splits the monolithic Base Station to Central/Distributed/Remote Units (CU/DU/RUs). As a consequence of the above, densification costs are driven down since the numerous RUs become functionally simple while computationally demanding functionalities are passed on to the more centralized CU and DU modules, which offer pooling advantages while providing enhanced flexibility to the MNOs [6]. However, the produced Fronthaul, i.e., the network between the CU and DU modules, and Midhaul, i.e., the network between the DU and CU modules, aggravate the RAN resource provisioning problem, as such connections must simultaneously support tremendous bandwidth, ultra-low latencies, and zero jitter [7]. In addition to the densification and adequate capacity provisioning issues, the nature of emerging 5G and industrial Internet applications that are classified under the Ultra-Reliable and Low-Latency Communications (URLLC) category pose severe latency constraints, which can be as low as 250 μs for factory automation applications [8]. From the above, it is evident that highly efficient converged FiWi RAN solutions that can support ultra-low latencies can play a critical role in the formation of the next-generation 5G RAN transport network.

Layer-2 protocol efficiency for converged FiWi networks has received much attention in recent years. FiWi networks are in general classified into two groups: (i) Radio-and-Fiber (R&F) and (ii) Radio-over-Fiber (RoF). In R&F networks, the two distinct optical and wireless media are being addressed separately, forming two discreet networks, each one implementing its own MAC layer scheduler with protocol translation transpiring at their interface. As a direct consequence of the above, the wireless MAC frames are transmitted solely in the wireless network segment and do not have to traverse the optical fiber to/from the centralized location, therefore avoiding the fiber propagation delay impact. However, R&F networks are applicable only in Decentralized Radio Access Networks (D-RANs), which are inefficient for use in dense urban areas with highly concentrated traffic requirements and more frequent site expansion and densification needs. The above is due to the necessity to deploy multiple antenna sites in close proximity, which dictates the need for having simpler APs with centralized control to ensure proper coordination [9].

Regarding RoF networks, initial works focused mainly on the wireless Layer-2 protocol functionality while considering predominately only the fiber length in their performance analysis. In [10], the authors studied the application of the 802.11 Point Coordination Function (PCF) and proposed a modification specifically targeting broadcast distributed antenna systems where multiple Remote Antenna Units (RAUs) are employed to serve as the antennas of a single AP, taking into account in their system model the added propagation delay due to the fiber connection between the RAUs and AP. The use of Analog-RoF (A-RoF) techniques for converged FiWi networks has received high research interest due to its high spectral efficiency benefits and the low complexity needed at the RAUs [11]. Nevertheless, A-RoF FiWi networks necessitate the joint study of the optical and wireless domains in order to offer optimal end-to-end performance. Consequently, new efficient medium-transparent protocols capable of optimally allocating both wireless and optical resources should be designed. To that end, in [12], a Medium-Transparent-Medium Access Control (MT-MAC) protocol was proposed for the first time for converged FiWi networks exploiting A-RoF, which efficiently manages both optical and wireless resources dynamically. In MT-MAC, the Central Office (CO) communicates directly with the MT-

MAC nodes (clients), without the intervention of the RAUs. As a result, the spectrum allocation decision takes place at the CO, i.e., the CO allocates the optical resources to the RAUs and the wireless resources to the users. In MT-MAC, the data traffic exchange is divided into Superframes (SFs), which contain two types of frames: (i) contention frames used for initial connection setup and status reporting and (ii) the frames containing the actual data exchange. In the initial form of MT-MAC [12–15], the SF size constituted a fixed number of transmission slots, which were the same for all RAUs, regardless of the number of active users served by each RAU at each time instance. With this scheme, resource allocation fairness among RAUs was the predominant target, and hence, all RAUs were allocated transmission windows of the same size by the CO to grant to their users independently of pending traffic. Focusing on the same MT-MAC version, in [16], a wireless multi-channel resource allocation technique was proposed for 60 GHz RoF local access networks, which takes into account predictions on the residual capacity of each wireless channel to reduce the handover latency. In [17], a method targeting at the reduction of the number of polling packets required to identify all active users was presented. A first attempt to provide Quality-of-Service (QoS) characteristics to the MT-MAC protocols was performed in [18], with the introduction of the QoS-aware Medium-Transparent (QMT) resource management scheme, which considered the existence of various traffic classes per node, with each traffic having a distinct priority attribute. In all these cases, however, a fixed transmission window is granted to each RAU, while specifically in the case of [18], the various traffic classes are also granted a static portion of the static transmission window. However, the mobility of wireless users essentially causes wide fluctuations in the RAUs' load over time, leading to inefficient spectrum usage under a fixed transmission window due to the high number of idle slots. To this end, a more sophisticated MT-MAC version, called Client-Weighted MT-MAC (CW-MT-MAC), was proposed in [19]. In this protocol, the CO grants transmission windows to each RAU proportional to the number of active users. Although CW-MT-MAC was able to achieve fairness among the network users, it still did not consider the actual traffic load of each RAU, as an RAU with more users could in total have lower aggregate traffic load than an RAU with few users being heavily loaded. Motivated by the need for a per-packet-based optical/wireless resource allocation, a traffic-aware MT-MAC scheme, termed gated-MT-MAC (gMT-MAC), was recently proposed [20], which employed the gated service paradigm for establishing the SF duration so as to maximize the network performance and spectrum efficiency. The gMT-MAC protocol, where each active user is authorized to transmit in an SF the amount of data it reports at the end of the previous SF, was shown to greatly outperform the original MT-MAC [12], as well as the CW-MT-MAC protocols [19] and achieve up to 20-times higher throughput, 2-times lower delay, and 5-times higher data wavelength utilization.

However, in the context of disaggregated RANs, the future transport networks are expected to provide connectivity solutions for a combination of Fronthaul/Midhaul/Backhaul (X-Haul) traffic, as the MNOs will wish to exploit the flexibility to deploy all sorts of equipment combinations: from the predominant Centralized Unit/Distributed Unit/Remote Unit (CU/DU/RU) split, to the CU/DU + RU split, i.e., the CU is separated through the Midhaul connection to the joined DU and RU equipment, as well as the legacy all-in-one CU + DU + RU formations, i.e., a monolithic Base Station. The above combinations signify that Layer-2 protocols employed in the future FiWi RAN transport networks must support Backhaul/Midhaul and Fronthaul connections, while concurrently meeting their distinct bandwidth, latency, and jitter Key Performance Indicators (KPIs). The gated service regime implemented in the State-of-the-Art (SoA) gMT-MAC protocol [20] does not offer service classification or a way to prioritize packets within the SF, and hence, packet flows originating from X-Haul equipment are served identically; to this end, the gMT-MAC protocol cannot effectively accommodate multiple traffic classes featuring their aforementioned diverse bandwidth, latency, and jitter specifications. To this end, this paper proposes the QoS-aware MT-MAC (qMT-MAC) protocol, which is specifically designed to provide the necessary performance guarantees to the various flows that are expected to traverse the

next-generation 5G and beyond transport networks, offering QoS support for three X-Haul traffic classes: (i) low-layer split Fronthaul (FH) traffic that produces Constant Bit Rate (CBR) loads and carries strict delay and jitter requirements, (ii) low-layer split FH that produces load-dependent traffic that carries strict delay requirements, and (iii) higher-layer split traffic that produces load-dependent traffic with more relaxed service constraints in terms of delay.

The rest of the paper is organized as follows: In Sections 2 and 3, the system model and the operation of the proposed qMT-MAC protocol are described, respectively. In Section 4, the performance evaluation and simulation results of qMT-MAC compared to the SoA are presented. Finally, Section 5 concludes the paper.

2. System Model

We considered a FiWi 5G RAN transport network in a Point-to-Multipoint formation, meaning the topology comprises a single central location connected to multiple remote locations, as depicted in Figure 1. At the central location, the MNO places the centralized equipment, which, depending on the level of disaggregation, can be either a 5G-Core unit, a Base Band Unit, a CU, or a CU + DU module. The centralized MNO equipment is connected through an Ethernet connection to the qMT-MAC CO with protocol translation taking place at their interface. The CO in turn extracts the Ethernet payload, inserts it into qMT-MAC packets, and modulates the latter on top of A-RoF carriers, which in the downstream traverse the optical fiber towards the RAUs. The RAUs transmit the wireless signal towards the qMT-MAC nodes, which in turn are connected through Ethernet to the MNO's remote equipment. Depending again on the disaggregation level, the remote equipment can be either a 5G Base Station (gNodeB/Small Cell), a DU+RU module, or an RU module. The qMT-MAC equipment is assumed to be mounted on top of street furniture, such as street light lampposts, since this is the predominant model considered for facilitating the RAN densification and installing the necessary Small Cells and other MNO remote equipment. However, the lamppost antennas are used here solely as an illustrative example, as in general the qMT-MAC nodes are considered to be collocated with the MNO remote equipment. A collection of data wavelength pairs is considered, with one wavelength from the pair used for Uplink (UL) and the other used for Downlink (DL) communication. In this way, the qMT-MAC fiber portion of the network operates under a Wavelength Division Multiplexing (WDM) scheme, allowing many wavelengths to be sent over the same fiber at the same time, resulting in higher field-fiber resource utilization efficiency. A dedicated wavelength pair is also employed as a common control channel, via which all control information is sent, while data wavelengths are primarily used for data packet exchange. Wireless communications on the UL and DL use distinct frequencies. In this work, without loss of generality, we focus on the UL traffic generation, i.e., from the nodes towards the mobile gateway. As shown in Figure 1, the wavelength allocation is considered to employ a wavelength selectivity device at each RAU, such as a Reconfigurable Optical Add–Drop Multiplexer (ROADM) or a Wavelength Selective Switch (WSS). These types of devices have been shown to offer very fast switching speeds that lie in the order of a few μs down even to a few tens of ns [21–23]. This enables dynamic network capacity reconfiguration based on actual load, resulting in an increased optical wavelength utilization factor. Because optical wavelengths are only allocated when pending traffic exists, higher energy- and cost-efficiency are also attained. It is worth mentioning, however, that the proposed protocol works independently of the wavelength switching speed. However, the faster the wavelength switching speed, the lower the additional switching overhead on the packet delay and, as a result, the greater the protocol performance is.

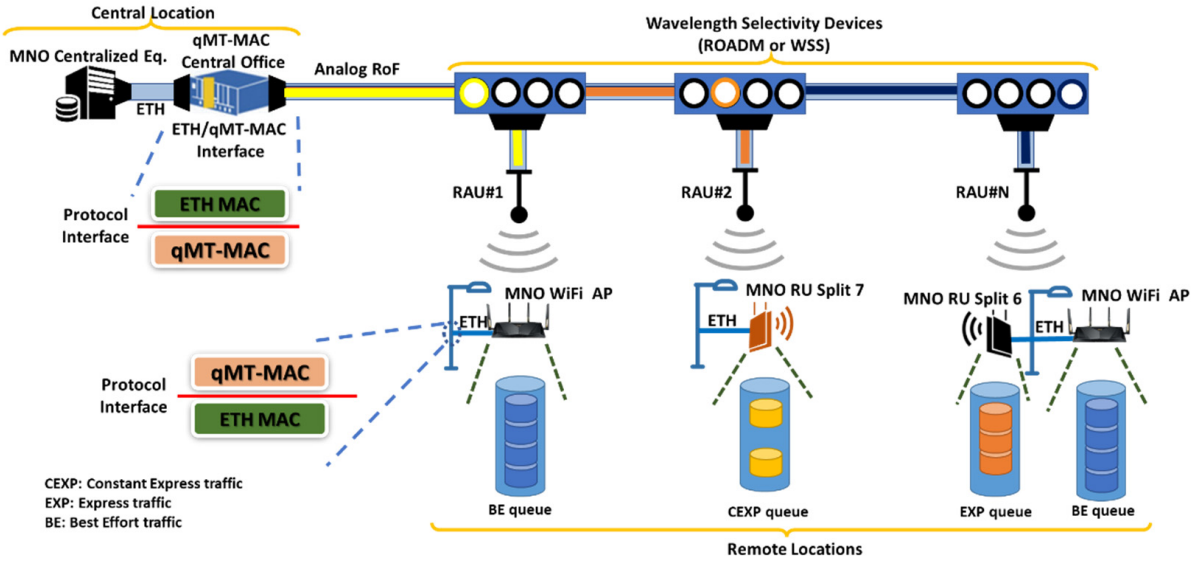


Figure 1. System model depicting the Point-to-Multipoint topology of the qMT-MAC A-RoF transport network: the MNO centralized equipment is connected to the qMT-MAC Central Office, while the MNO remote equipment is connected to the qMT-MAC nodes.

The Ethernet-based communication between the MNO equipment and FiWi qMT-MAC network facilitates the use of enhanced Common Public Radio Interface (eCPRI) messages for data exchange as the predominant protocol for X-Haul communication. In order to encompass and simulate the main eCPRI splits in our study, we considered that the MNO equipment produces the following three types of payloads:

- Constant Express traffic (CEXP): This type of traffic simulates a low-split FH traffic that has strict delay and delay jitter constraints. Examples of this kind of traffic are the 3GPP splits 7 and 8. The traffic pattern exhibited by these splits is the Constant Bit Rate (CBR), which does not fluctuate with the number of users present in the cell [24]. According to the eCPRI specifications, CEXP traffic needs to support delay up to 100 µs and jitter up to 65 ns [25].
- Express traffic (EXP): This type of traffic still simulates FH traffic with strict latency constraints, but belongs to other popular higher FH splits, i.e., 3GPP split 6, with load-dependent traffic pattern [25]. In this paper, we considered that EXP's exhibited delay must be up to 250 µs, following 3GPP's specification [8]. In our work, we also considered a Self-Similar traffic model for packet arrivals for EXP traffic. The reasoning and explanation behind the use of this Self-Similar model for the load-variable split 6 traffic is presented in Appendix A.
- Best Effort traffic (BE): This type of traffic simulates all other types of traffic that have relaxed timing constraints. For instance, this type of traffic can represent 3GPP splits that are higher than split 6 and other Backhaul traffic. The BE traffic is load-dependent and also follows a Self-Similar model.

Please note that regarding data packets, the terms "packets" and "frames" are used interchangeably throughout this paper. Finally, it is considered that each lamppost antenna can host more than one traffic-producing entity, by combining the equivalent number of Ethernet Network Interface Cards, as shown on the lower right-hand side of Figure 1.

3. The QoS-Aware MT-MAC Protocol

Section 3.1 summarizes the general operational rules of the SoA MT-MAC protocols presented in [12,19,20] that are in direct relation to the medium arbitration process, using the more recent gMT-MAC protocol as an example [20]. A more detailed and in-depth description of these protocols is provided in the respective references. Sections 3.2 and 3.3 proceed with describing the qMT-MAC protocol proposed in this paper, which, as opposed

to the works presented in [12,19,20], introduces additional features capable of offering flow prioritization and QoS features for delegation of X-Haul traffic.

3.1. State-of-the-Art MT-MAC Protocol Operational Rules

All data interchange is managed by the CO, which is connected via fiber to a number of RAUs, which in turn give wireless connectivity to the lamppost units, according to the protocol's specifications. Two separate Contention Periods (CPs) are used to accommodate the medium's dual nature: the first CP seeks to distribute optical wavelengths across RAUs currently serving active wireless nodes, while the second CP allocates wireless capacity among them. The CO produces a short beacon pulse on a specially dedicated channel known as the Control Channel at the start of the first CP, which is then broadcast to all in-range wireless nodes. When nodes detect the pulse, they quickly respond with a brief pulse of the same duration, if they contain pending data to transmit in their buffers. The CO determines which RAUs contain active nodes and, consequently, assigns wavelengths to them by collecting the received pulses based on the energy detection method [26] and calculating the time difference between their receptions to identify the originating RAU based on the reception window, as shown in Figure 2. If the number of RAUs containing active nodes is greater than the number of available wavelengths in the system, the wavelengths are cycled through the RAUs using a Round Robin algorithm.

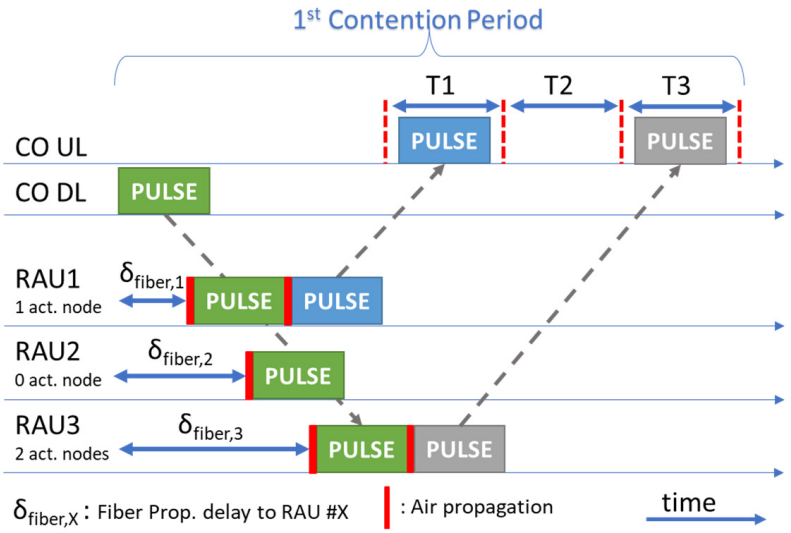


Figure 2. First Contention Period example for determining which RAUs contain active nodes. Based on reporting pulses' arrival times, the CO can detect which RAUs contain active nodes and which do not. In the example above, RAUs 1 and 3 contain active nodes.

The CO starts the second CP, which is logically divided into SFs, after obtaining the complete list of capacity-demanding RAUs. An SF contains two independent and non-intermixing sets of frame types: Resource Request Frames (RRFs) and Data Frames (DFs), with the RRFs always coming first. The DFs are in charge of real data transmission, whereas the RRFs provide the CO with information about the number and IDs (i.e., MAC addresses) of each specific node before any data exchange can begin, essentially acting as service setup protocol exchange. As seen in Figure 3a, the RRFs are further subdivided into groups of m slots, with each slot containing POLL, ID, and ACK packets in the order specified. Each active node chooses a random integer value y in the interval $[0,\ m]$ at the start of each RRF, where y is the number of POLL packets that must be received, before replying with an ID packet that contains the node's MAC address and its Buffer Status (BuS), i.e., how many packets are present in the nodes' buffers. In the best-case scenario, each node selects a distinct y value and transmits its own ID packet in its own slot. The CO responds with an ACK after receiving the ID + BuS packet correctly, indicating that this node has been successfully recognized and should not participate in any additional

RRFs. A collision happens when two or more nodes choose the same value for y, and as a result, the CO does not send an ACK, forcing these nodes to participate in the next RRF, which follows soon afterwards. The CO continues to send RRFs until no collisions occur, thereby indicating that all active nodes have been identified and the second CP has come to an end. The CO then commences the DATA_TX phase, during which the major data exchange takes place in the form of a sequence of DF broadcasts until the SF ends. In order to update their BuS to the CO, nodes will piggyback their BuS information into the last DF transmission of the current SF and will therefore not partake in any subsequent second CP that will be initiated by the CO. The CO periodically initiates new second CPs, as a means for previously inactive nodes to report their status and be thusly included in the upcoming SF. Note that, because of the explicit polling nature, no inter-frame spaces are assumed to exist between the transmitted packets, leading to higher medium utilization efficiency, while the DFs and RRFs are properly ordered by the CO in the time domain to be of equal duration.

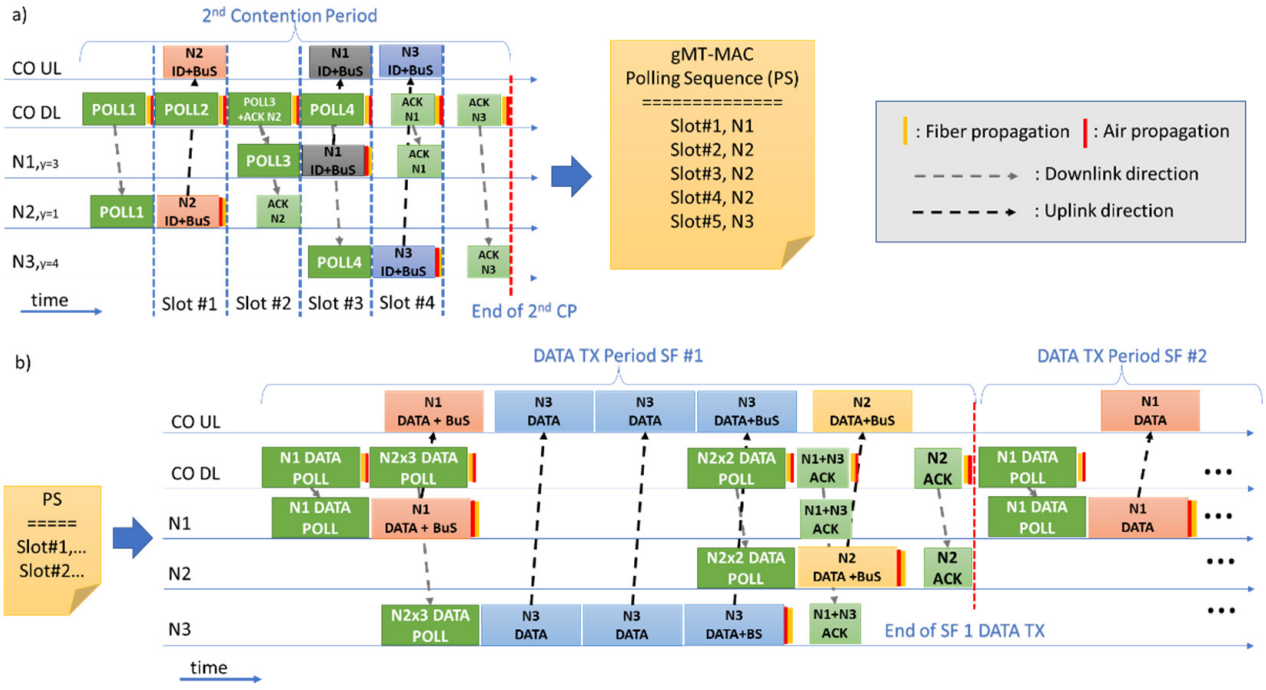


Figure 3. Operation of the legacy gMT-MAC protocol. (**a**) An example of the 2nd Contention Period operation for an RAU with 3 connected nodes. Each node chooses randomly the slot to transmit its MAC address (ID) and Buffer Status (BuS). If there are no collisions, the CO transmits an ACK packet acknowledging the correct reception of the ID + BuS packets. Based on the latter, the CO constructs the Polling Sequence (PS) of the next SF. (**b**) DATA_TX period example for an RAU with 3 nodes, with N1 having 1 packet to transmit, N2 having two packets to transmit, and N3 having 3 packets to transmit.

Each DF comprises the exchange of DATA_POLL, DATA, and ACK packets as depicted in Figure 3b. DATA_POLL packets denote which MT-MAC client has authorization to transmit immediately after the reception of the DATA_POLL message. Following the DATA_POLL reception, the MT-MAC node transmits the data packets as instructed and, finally, the CO transmits an ACK packet to the node to acknowledge the correct data reception. DATA_POLL packets are created as per the Polling Sequence (PS) that is constructed by the CO at the end of the second CP, defining the transmission schedule of each SF. The algorithm that creates the PS depends on the specific version of the MT-MAC protocol. For instance, in the original MT-MAC protocol [12], the PS has a predefined size, which is divided equally amongst the active RAUs. In the CW-MT-MAC protocol [19], each active user recognized by means of the second CP is assigned a predefined number of packets in

the PS. Finally, in the gMT-MAC protocol [20], the PS is constructed based on the number of packets the nodes have reported during the first CP, and each client receives a transmission opportunity window that is equal to the time necessitated for transmitting the number of reported packets. The PS creation algorithm for the proposed qMT-MAC is described in Section 3.2. Nodes that have successfully advanced to the DATA_TX period can piggyback their BuS at the end of their final DATA packet, thus avoiding the necessity to partake in a subsequent second CP.

3.2. The QoS-Enabled MT-MAC

This section presents the proposed QoS-enhanced version of the MT-MAC protocols, termed qMT-MAC, specifically designed to offer QoS functionalities to the MT-MAC protocols, in order to be able to support all the traffic types present in 5G RAN transport networks, as explained in Section 2. With respect to the 1st and 2nd CPs, the qMT-MAC protocol follows the same operational rules as the previously described MT-MAC protocols. However, as opposed to the PS creation policies described in Section 3.1, the qMT-MAC protocol devises the PS by examining and prioritizing the flows based on their classification into three categories: Constant Express traffic (CEXP), Express traffic (EXP), and Best Effort traffic (BE). Classification of the packet flows takes place by examination of Layer-2 header fields, such as the "Ethertype" field, or the VLAN tag or the source MAC address, denoting the type of equipment that is producing the X-Haul traffic and what class this traffic belongs to. To this end, each qMT-MAC client is considered to contain up to three queues, i.e., one for each traffic category.

In qMT-MAC, the nodes transmit their BuS using the ID packets to the CO prior to the initiation of the DATA-TX phase, as done in the gMT-MAC, with the difference being that, in the proposed qMT-MAC, they transmit the kind of traffic as well (CEXP, EXP, or BE). Hence, in qMT-MAC, the CO knows not only the number of packets each node has, but also receives their classification to the three aforementioned traffic categories. The above functionality is shown in Figure 1, where the qMT-MAC nodes are providing access to a set of RUs and WiFi AP devices, with each device producing a different kind of traffic (RUs being 5G FH equipment producing either CEXP or EXP traffic, whereas WiFi APs produce BE traffic). qMT-MAC operates in a slotted time base, with the slot duration set so as to adhere to the transmission delay of an ETH Maximum Transmission Unit (MTU) of 1500 bytes plus 18 header bytes, resulting in the maximum frame size of 1518 bytes.

The creation of the qMT-MAC PS takes place in four stages, as depicted in Figure 4:

- The first stage targets scheduling and combining the CEXP packets in such a pattern that the delay jitter, i.e., the interval between any two consecutive packets of the same CEXP flow, is ideally zero without producing conflicts amongst the different CEXP flows. Since CEXP traffic is CBR in nature, the CEXP transmission schedule is calculated once the CEXP nodes have been identified and their allocation in the PS is copied into every subsequent SF.
- The second stage inserts EXP packets in the remaining empty slots after the inclusion of the CEXP packets in the PS. The EXP packets are sequenced in a Round Robin fashion so that the delay is distributed evenly among the different EXP queues that are of the same priority. EXP packets that did not fit into the current SF will be inserted in the PS of the next SF.
- During the third stage, the BE packets are inserted into the remaining empty slots of the PS (if any) in a sequential manner, i.e., BE packets are grouped in the PS based on their MAC address or, equivalently, their originating queue. The latter sequencing follows a method to potentially have contiguous BE slots addressing the same qMT-MAC client. This functionality allows the qMT-MAC to implement advanced EXP packet priority policies, such as pre-emption, which are detailed later in the section. BE packets that did not fit into the current SF will be inserted in the PS of the next SF.
- During the fourth stage, the remaining empty slots in the PS (if any) are released for BE packet transmission even if there are no more pending BE packets after the third

stage. Again, these added BE slots are placed in a sequential manner for the same reason as explained in the third stage.

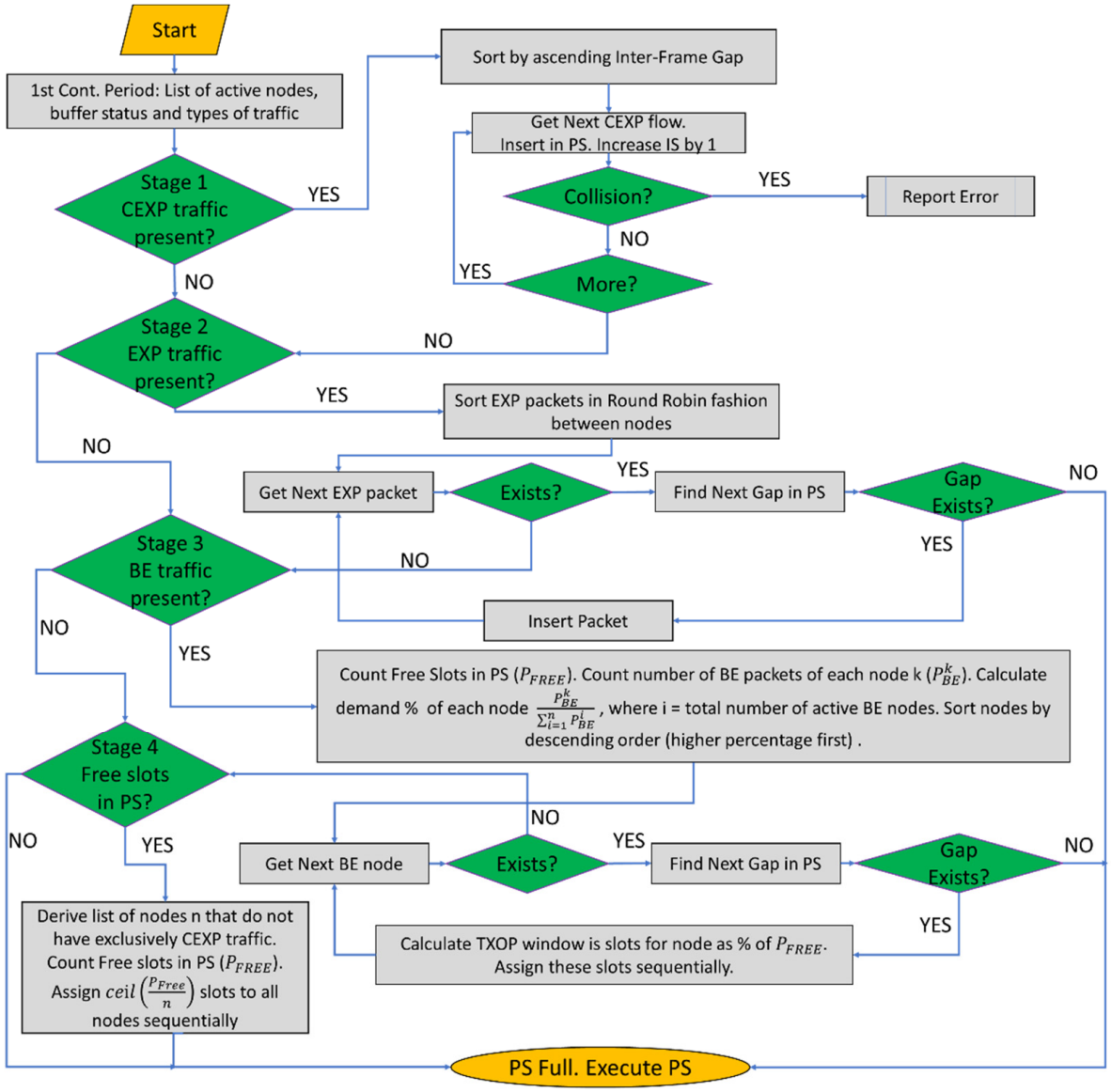


Figure 4. Polling Sequence creation algorithm for qMT-MAC.

The insertion and prioritization of the CEXP traffic is based on the CEXP-Fit algorithm presented in Table 1.

Table 1. The CEXP-Fit algorithm.

Step #	*Action*
Step 1:	*Identify each flow* $F_i = \{IFG_i\}$, *where* IFG_i = *Inter Frame Gap of flow* F_i *(in slots). The duration of the Superframe denoted as TSF is calculated as the Lowest Common Multiple (LCM) of IFGx values of all flows.*
Step 2:	*Flows are arranged in an array based on the ascending order of IFG.*
Step 3:	*Lowest IFG flow inserted first at slot 1* $IS_i = 1$ (IS_i = *Initial Slot of flow i in SF). Slots of the form* $IFGi \cdot m + IS_i$, $m = 0, 1, \ldots$ *are removed from the set of available slots. Next flow offset to next available IS slot.*
Step 4:	*Next flow in ascending order is inserted at* IS_i. *Step 4 is repeated until all flows have been inserted into the PS.*

Each CEXP flow F_i is characterized by its Interframe Gap IFG_i measured in slots. Flows are arranged in ascending order of $IFGi$. The duration of the SF T_{SF} is calculated based on the Least Common Multiple (LCM) of all IFG_i. Flow F_i with the lowest IFG_i is inserted in slot 1 of the PS. The first slot of every flow F_i is termed its Initial Slot IS_i Consequently, slots of the form $IFG_i \cdot m + IS_i$, $m = 0, 1 \ldots$ are removed from the set of available slots of the PS. The algorithm continues with the next flow, which is shifted to the first available slot of the PS, until all CEXP flows have been inserted into the PS. For the CEXP flows, we assume the following:

$$\sum_{i=1}^{N} \frac{1}{IFG_i} \leq 1, \; where \; N \; = \; number \; of \; CEXP \; flows \tag{1}$$

$$For \; every \; two \; flows \; F_i, F_k, \; it \; must \; hold : IS_i - IS_k \; \neq \; n \cdot (IFG_i \; - \; IFG_k). \tag{2}$$

Equation (1) ensures that the network is not oversubscribed, whereas Equation (2) states that for every two flows F_i and F_k, the difference of their initial slots IS_i and IS_k should not be a multiple of the difference of their IFGs since this would result in a collision. Figure 5 shows an example of the result of the CEXP-Fit algorithm described above for three flows F_1, F_2, and F_3 with IFGs of 4, 8, and 16 slots, respectively.

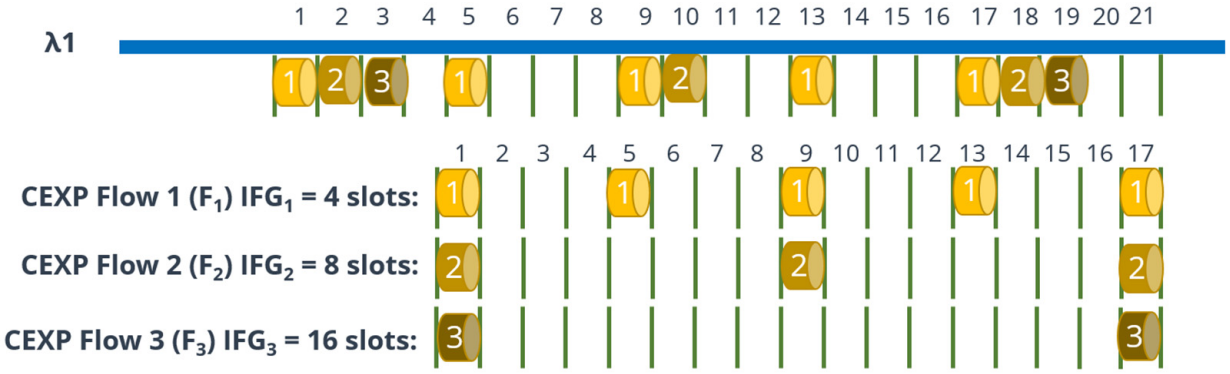


Figure 5. Example operation of the CEXP-Fit algorithm for 3 CEXP flows with IFGs of 4, 8, and 16 slots, respectively.

3.3. Express Traffic Priority Enhancements in qMT-MAC

The PS creation sequence of the qMT-MAC protocol provides a clear priority to CEXP and EXP traffic, since packets of this type are always placed first in the PS, while BE packets are inserted in the PS only after the insertion of the CEXP and EXP traffic. However, since delay-bounded EXP traffic can arrive within the duration of an SF, i.e., while the network is executing a specific PS, the newly arrived packet is forced to wait until the next SF is transmitted, causing delays that could be detrimental to X-Haul or URLLC traffic. To this end, the qMT-MAC protocol proposes two additional priority policies for nodes that combine EXP and BE queues, as displayed on the lower right-hand side of Figure 1, to further enhance the EXP traffic priority over BE traffic. In total, a qMT-MAC client serving both EXP and BE traffic will execute the PS according to one of the following three PS execution policies:

1. Default priority PS execution policy: This is the default policy, under which the qMT-MAC client follows the PS as it is constructed by the CO based on the PS creation algorithm shown in Figure 4. Under this regime, when a client receives a DATA_POLL for BE traffic, it checks the status of the BE queue, and in case there is a pending packet, the packet is transmitted. If the BE queue is empty, the client checks its EXP queue, and if an EXP packet is located there, it gets transmitted. Otherwise, the transmission slot remains empty.
2. EXP priority PS execution policy: Under this policy, when the qMT-MAC client receives a BE DATA_POLL, it checks the EXP queue first for outstanding packets, and

if one is found, it gets transmitted instead of the BE packet. If no EXP packets are waiting for transmission, only then does the client proceed in polling the BE queue for packets.

3. Pre-emption priority PS execution policy: This scheme is similar to the previous policy, since the client always polls the EXP queue first for a packet to transmit. If the EXP queue is empty, then it polls the BE queue. In addition, this scheme considers also packet pre-emption, meaning that when an EXP packet arrives and the medium is busy due to the on-going transmission of a BE packet, the queuing system allows the EXP packet to disrupt the transmission of the BE packet, pending the preemptable frame having at least 60 bytes already transmitted and at least 64 bytes still remaining until the end of the preemptable frame is reached [27]. Packet pre-emption has become increasingly important lately, since it was shown that a severe delay may be caused by starting a large, low-priority frame ahead of a time-critical frame [28]. Packet pre-emption has been adopted and standardized in the IEEE 802.3Qbr and 802.3Qbu standards, which deal with Time-Sensitive Networking [29,30], and has been shown in various works in the literature to further reduce the average delay of the EXP traffic, while also reducing the observed delay jitter [27,28].

4. Results

In order to assess the performance of qMT-MAC and its ability to combine CEXP, EXP, and BE flows, while maintaining the strict Fronthaul standards, a performance evaluation based on the OMNET++ simulator [31] was carried out. The evaluation was performed against the SoA gMT-MAC protocol in order to assess the improvement with respect to throughput, delay, delay jitter, and packet drops for X-Haul traffic patterns falling under the CEXP, EXP, and BE categories. The network setup follows the schematic of Figure 1, while the full simulation specifications are presented in Table 2.

Table 2. Simulation parameters.

Parameter	Value
Speed of light in fiber	2×10^8 m/s
RAU range	50 m
Air propagation delay	0.2 μs
Bit rate per wavelength	1 Gbps
Data packet size	1512 Bytes
ID packet size	72 Bytes
POLL packet size	72 Bytes
ACK packet size	16 Bytes
Fiber length	1–10 km

Figure 6 displays the performance evaluation of qMT-MAC vs. the SoA gMT-MAC protocol for three CEXP flows vs. fiber length. The three combined CEXP flows have IFG 4 (normalized load 25%), IFG 8 (normalized load 12.5%), and IFG 16 (normalized load 6.25%), respectively, totaling an aggregated load of 43.75% at the network. Normalized load corresponds to the produced payload as a percentage of the Channel Bit Rate, i.e., a 0.1 normalized load corresponds to payload generation equal to 10% of the Channel Bit Rate, etc. As our work targets dense urban environments, the tested fiber length ranged from 1 km up to 10 km, with a step of 1 km. As can be observed in Figure 6a, throughput was always constant, as expected from CBR traffic sources, and both qMT-MAC and gMT-MAC achieved similar performance in terms of throughput, managing to steadily output all incoming CEXP traffic flows. However, examination of Figure 6b reveals that the two protocols exhibited different behaviors in terms of average packet delay and delay jitter of the latter. In the case of qMT-MAC, delays for all three flows exhibited a linear increment with fiber length as the propagation delay adds a constant delay of 5μs per km. In all tested cases and for fiber lengths up to 10 km, all three CEXP flows exhibited delays that

consistently remained lower than the target value of 100 μs set by the eCPRI standard. By means of Figure 6b, it can also be seen that flows with higher IFGs (lower load) exhibited higher delay compared to the flows with lower IFG values (higher load). This is due to the CEXP-Fit algorithm utilized in qMT-MAC, which prioritizes flows with a lower IFG (higher load) while shifting each flow with a lower IFG by one packet transmission delay, thus attributing a constant delay difference amongst each flow. The simulation results also showed that in the case of qMT-MAC, the delay jitter for all three CEXP flows was always zero, again meeting the strict requirements set by the eCPRI standard. This is due to the fact that in qMT-MAC, CEXP flows have reserved slots in the PS, and therefore, the protocol manages to guarantee service delivery at a stable rate, while respecting the strict delay and delay jitter requirements. In the SoA protocol gMT-MAC, however, we noticed that average delay values increased faster with added fiber length, while the rate of increment depended on the IFG value, i.e., the load of the flow. Specifically, we observed that CEXP flow with IFG 4 (normalized load 25%) increased faster with fiber length as opposed to CEXP flow with IFG 8 (normalized load 12.5%), which in turn increased at a faster rate than the CEXP flow with IFG 16 (normalized load 6.25%). This was attributed to the fact that the longer fiber lengths led to a higher SF duration, which in turn allowed for more packets to be generated by each node before the start of the next SF. As more packets reside in the node buffers, it took more time for these packets to reach the head of the queue, thus increasing the average packet delay. Flows with a lower IFG (higher load) produced more packets, and therefore, these flows exhibited higher delay increment rates. As a result, it was observed that while CEXP flows with IFGs of 8 and 16 maintained an average packet delay lower than the target of 100 μs, the CEXP flow with IFG4 did not and surpassed the above target even at 1 km of fiber length. The greater service time for packets that reside at the back of the queue was also attested by the vertical error bars denoting the delay jitter, confirming that as fiber length (and, consequently, the SF duration) increased, more packets were generated, and packets at the back of the queue experienced higher delays than packets that were at the front of the queue, inevitably leading to higher delay jitter values, which started at around 20 μs at 1 km of fiber, reaching up to 75 μs at 10 km of fiber. The above discussion showcases that gMT-MAC's gated service policy cannot meet the eCPRI Key Performance Indicators (KPIs) for low-layer CBR FH traffic, both in terms of delay (100 μs) and delay jitter (65 ns), whereas the reserved time slot qMT-MAC policy managed to obtain both goals, offering delay values that increased only due to the added propagation delay, while exhibiting zero delay jitter. In this test, all flows for both protocols exhibited zero packet drops, since the aggregated load of 43.75% of the test scenario could be served in a timely manner by both protocols and no buffer overflow events took place.

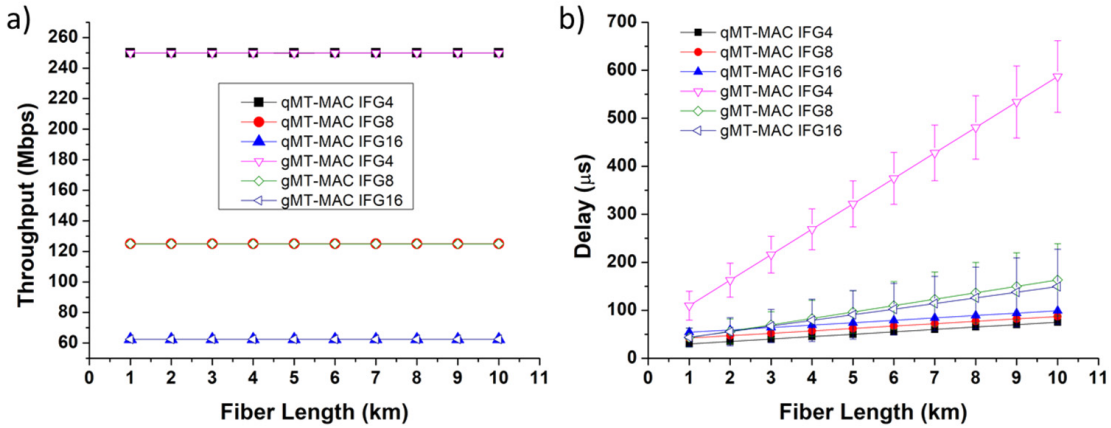


Figure 6. (**a**) Throughput vs. fiber length for three combined CEXP flows with IFG 4, 8, and 16, respectively, (**b**) Delay vs. fiber length for three combined CEXP flows with IFG 4, 8, and 16, respectively.

Figure 7 displays the qMT-MAC vs. the SoA gMT-MAC performance comparison for a combination of all three types of traffic versus load. Specifically, this test considered a

network with each wavelength being shared amongst three nodes, while each node serves a different flow type, i.e., one node serves a CEXP flow, one node serves an EXP flow, and one node serves a BE flow. CEXP traffic has an IFG of five, denoting a constant 0.2 (20%) normalized load generation, while the remaining 80% of bit rate capacity (800 Mbps) remains free for the EXP and BE flows. The fiber length was set at 1 km, and the normalized load displayed at the x-axis took values of 0.1–1.0 with a step of 0.1. In this test, the produced load refers to individual EXP and BE traffic, which were assumed to have the same load, i.e., the load in both EXP and BE flows increased concurrently. By means of Figure 7a, it can be seen that CEXP traffic had a constant throughput output for all loads under both protocols, since in the case of qMT-MAC, CEXP traffic is served in reserved time-slots, while in gMT-MAC, the Round Robin nature of served traffic means that no node is being led to starvation. With respect to EXP and BE traffic flows, however, we noticed that qMT-MAC and gMT-MAC differ greatly, as under gMT-MAC operation, EXP and BE were treated with the same priority and achieved the same plateau of 400 Mbps, while under the qMT-MAC protocol, once the aggregated produced traffic by both flows reached the remaining capacity of the channel at a normalized load of 0.4, EXP traffic flow was prioritized over BE traffic. Specifically, as the load continued to increase beyond 0.4, EXP traffic throughput increased linearly until it reached the maximum value of 800 Mbps. On the contrary, BE throughput decreased steadily as the load increased more than 0.4, since the network's capacity was absorbed by EXP traffic, leading the queue to starvation once the load reached 0.8 and beyond.

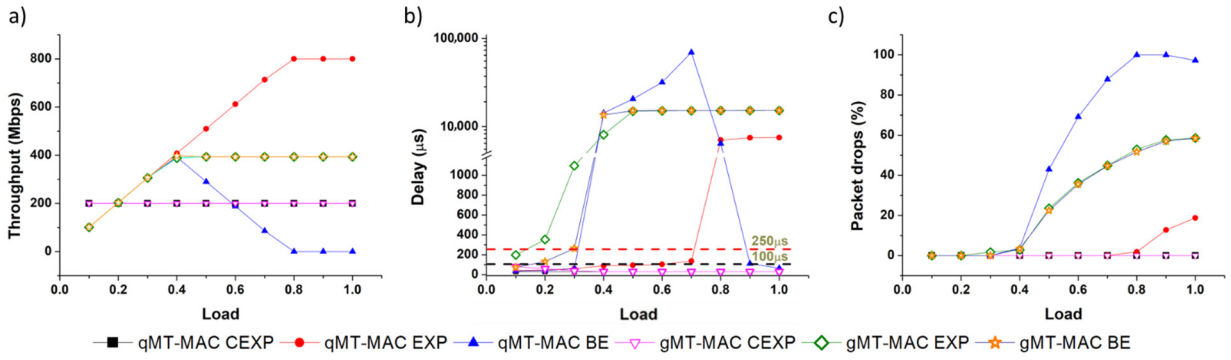


Figure 7. Performance evaluation vs. load for three combined flows (CEXP, EXP, and BE).

Figure 7b displays the average delay vs. load for both protocols and all traffic flows. It can be observed that CEXP traffic flows were served in a timely manner under both protocols, and the produced delays stayed below 100 μs for all loads, since qMT-MAC reserved the slots for CBR traffic, while gMT-MAC served nodes under the Round Robin paradigm; therefore, each node was guaranteed an equal portion of the Polling Sequence. However, again, we noticed that under gMT-MAC, EXP and BE packets were treated equally, resulting in both flows quickly surpassing the threshold of 250 μs at loads of 0.3 and above, with the delay reaching a maximum value of ~15 ms for all loads greater than 0.4. In the qMT-MAC case, however, EXP traffic increased at a very slow pace, and the produced results surpassed the 250 μs threshold only when the load approached 0.8, while, on the contrary, BE delay increased rapidly when the load increased above 0.3 and, at the highest point, reached values close to 100 ms. This performance difference is evident since EXP traffic has clear priority over BE traffic in the creation of the PS, and to this end, it is served quickly, achieving sufficient delay budgets for all loads less than the network's capacity. BE delay under qMT-MAC decreased when the load is greater than 0.7; however, this was due to the fact that only a handful of BE packets reached their destination in these high-load conditions (as confirmed by Figure 7c, discussed later on), and since the delay statistic was only measured for non-dropped packets, these few packets that remained took advantage of the very few transmission opportunity windows that came up following EXP packet drops, which were accounted for at loads greater than 0.8.

Finally, Figure 7c displays the percentage of packet drops for each protocol and each flow. The results in Figure 7c confirmed the results displayed in Figure 7a,b, showing that CEXP traffic flows exhibited zero packet drops for both protocols, while for the EXP and BE traffic classes, packet drops were in tandem and greater than zero for loads >0.4 under the gMT-MAC protocol due to buffer overflows. Under the qMT-MAC protocol, however, the EXP traffic class maintained a clear advantage, since the EXP traffic flow exhibited non-zero packet losses only when the load approached the system's capacity at 0.8, again due to buffer overflows, while for BE traffic, non-zero packet losses occurred and increased rapidly when the load surpassed 0.3 and reached up to 100% at load values of 0.7. Beyond a 0.7 load value, BE packet drops showed a limited decline, as at the same time, packet drops occurring in the EXP queue resulted in some infrequent gaps in the PS, which translated to transmission opportunity windows for the BE flow.

Figure 8 presents the performance evaluation of the qMT-MAC protocol under the three PS execution policies, aiming to further enhance the priority of EXP packets over BE packets, i.e., EXP priority and Pre-emption priority. This simulation considered a network where a node concurrently serves an EXP and a BE flow. Again, CEXP traffic has an IFG of five, denoting a constant 0.2 (20%) normalized load generation, while the remaining 80% of bit rate capacity (800 Mbps) remained free for the EXP and BE flows. The fiber length was set at 1 km, and the normalized load displayed at the x-axis took values of 0.1–1.0 with a step of 0.1. Similar to the results of Figure 7, the produced load refers to individual EXP and BE traffic, which were assumed to have the same load, i.e., both EXP and BE flows increased concurrently. Figure 8a presents the throughput performance results vs. load, while t 8b presents the packet drop percentage vs. load. As can be seen in both figures, results are grouped based on the type of flow, while the same trends as in the case of Figure 7 were observed. CEXP traffic exhibited constant throughput output and zero packet drops irrespective of the PS execution policy, while EXP flows gained priority over BE flows, resulting in a linear increase of the achieved throughput until the system's capacity was reached at a 0.8 load and packet drops started to occur. On the contrary, the lower priority of BE flows resulted in a throughput decrease and higher packet drops at loads higher than 0.4 when the aggregated CEXP/EXP/BE load reached the system's capacity. Figure 8c,d present the delay performance under the three PS execution policies for the EXP and BE flows, respectively.

By means of Figure 8c, it can be seen that for very-low-load values (0.1) the enhanced priority policies produced marginal benefits compared to the No priority policy. This was due to the fact that, in very-low-load conditions, the default priority scheme at the creation of the PS suffices to produce adequate prioritization as the low packet generation means that only a few EXP packets will arrive during an SF and will have to wait for the next PS. However, as load increased, we witnessed significant performance gains produced by the enhanced priority schemes, reaching up to 62.25% for the EXP priority and up to 64% for the Pre-emption policy vs. the equivalent No priority results. This performance improvement stemmed from the fact that under the EXP priority scheme, an EXP packet does not have to wait for the next PS to be transmitted and can, instead, take over the transmission slot of the next BE packet, while under the Pre-emption policy, an EXP packet can even interrupt the on-going transmission of a BE packet and gain even further performance improvement. By means of Figure 8d, it can be seen that the opposite was true for the BE flows, as the enhanced priority PS execution policies produced higher delays for the BE packets as the prioritization schemes further stalled their transmission. Therefore, it became evident that the enhanced priority policies could produce significant delay reductions for delay-sensitive traffic, making them more suitable for use with delay-bounded traffic such as FH or URLLC.

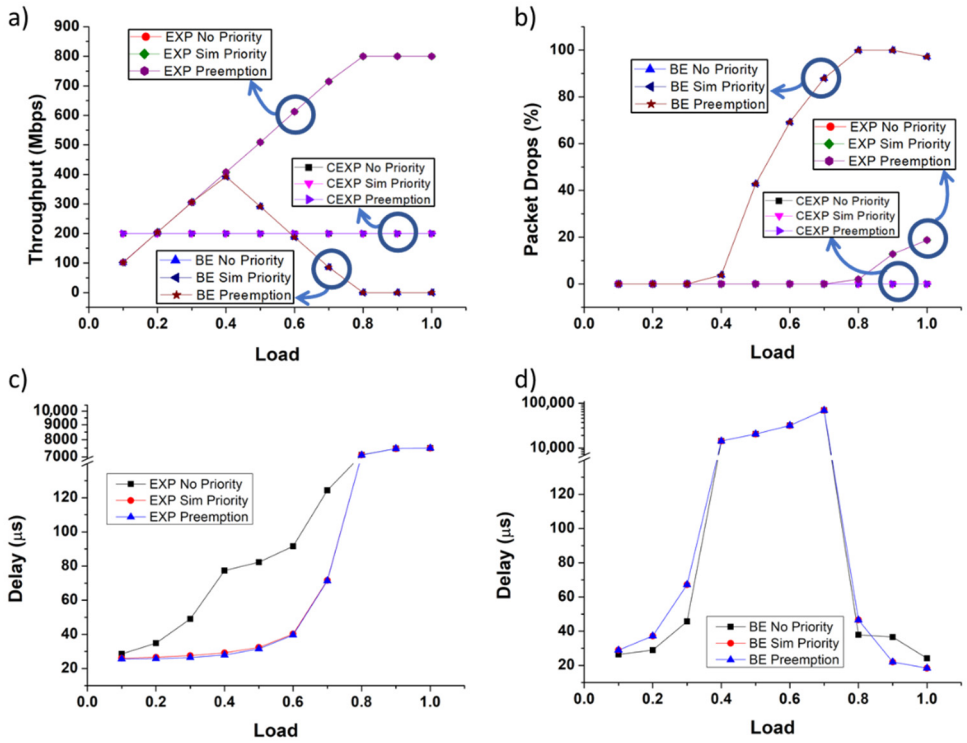


Figure 8. Performance evaluation vs. load for three PS execution policies: No priority, EXP priority and Pre-emption priority: (**a**) Throughput vs. Load, (**b**) Packet drops vs. Load, (**c**) Delay vs. Load for EXP traffic, and (**d**) Delay vs. Load for BE traffic.

5. Conclusions

In this paper, we proposed a QoS-enabled Medium-Transparent MAC protocol, termed qMT-MAC, for Fiber-Wireless A-RoF 5G transport networks. qMT-MAC was shown through simulations to efficiently support three types of services, i.e., Constant Express, Express, and Best Effort, under the same framework, while achieving the respective delay and jitter requirements set by the standards. Specifically, it was shown that, under qMT-MAC, the CEXP traffic flows can be optimally combined to satisfy the strict delay and delay jitter requirements set by the eCPRI standard. On the other hand, EXP traffic flows were shown to have significant prioritization and be able to maintain a <250 µs delay even for load conditions that approach the network's capacity. Finally, it was shown, that two additional proposed enhanced priority PS execution policies could offer significant performance gains, reaching up to a 64% reduction of attested delay for the Pre-emption policy vs. the Default priority scheme, overall solidifying qMT-MAC's ability to serve delay-sensitive traffic over the SoA MT-MAC protocols.

Author Contributions: Conceptualization, G.K. and N.P.; architecture design, G.K., N.P., D.P., C.V. and R.M.; methodology, A.M. and M.G.; simulator implementation, D.P. and M.G.; validation, A.M. and M.G.; resources, G.K. and A.M.; writing—original draft preparation, G.K. and D.P.; writing—review and editing, C.V., M.G., A.M., R.M. and N.P.; visualization, G.K. and A.M.; supervision, N.P. and G.K.; project administration, G.K., M.G. and A.M.; funding acquisition, G.K., A.M. and C.V. All authors have read and agreed to the published version of the manuscript.

Funding: This work was funded by H2020 5G-COMPLETE (GA 871900) and H2020 Int5Gent (GA 957403).

Institutional Review Board Statement: Not applicable.

Informed Consent Statement: Not applicable.

Data Availability Statement: No new data were created or analyzed in this study.

Conflicts of Interest: The authors declare no conflict of interest. The funders had no role in the design of the study; in the collection, analyses, or interpretation of the data; in the writing of the manuscript; nor in the decision to publish the results.

Appendix A. Stochastic Self-Similar Traffic Models

It has long been established, via statistical analysis of captured live network traces, that Poisson-based traffic models are not always realistic, and in fact, real network traffic exhibits Self-Similar (SS) fractal properties, which necessitates the use of more advanced traffic models. This observation was first made in [32] for Ethernet traffic captured within a Local Area Network (LAN) environment (also containing traffic originating or destined for hosts outside the LAN) and was later confirmed also for Wide Area Network (WAN) settings [33], particularly for Variable Bit Rate video-dominated data [34], as well as for Wireless LANs [35]. Intuitively, the self-similarity property exhibits itself as a statistical trendm, which does not diminish when averaged over increasing time scales, as is the case in Poisson processes, thus leading to increased "burstiness" compared to non-self-similar traffic. Furthermore, the aggregation of multiple self-similar traffic streams typically strengthens the self-similar property of the overall traffic and increases its burstiness, which leads to higher queueing delays and presents additional challenges to QoS provisioning.

The cause of the emergence of self-similarity was identified in [32] as the fact that, in real network traffic, the inter-arrival frame/packet (depending on the examined layer) distribution is heavy-tailed, allowing for very large inter-arrival times with significant probability. Although numerous heavy-tailed distributions exist and have been studied, the Pareto distribution parameterized by a parameter α, with $1 < \alpha < 2$, is the one most commonly proposed in the networking literature [36,37]. Specifically, the Pareto parameter α for the inter-arrival time distribution is related to the Hurst exponent H of the resulting self-similar stream as $H = (3 - a)/2$.

The detailed statistical analyses performed on network traces have yielded H values in the range 0.65–0.8, depending on the time of day (i.e., busy-hour vs. breaks) [32,38] and even the employed transport layer protocol [34]. Specifically, the congestion control of the Transmission Control Protocol (TCP) creates a highly varying instantaneous rate, leading to higher values of H compared to the User Datagram Protocol (UDP). For these reasons, it is more appropriate to examine the network performance over the entire range of 0.65–0.8 of H (which corresponds to α Pareto parameters in the range of 1.4–1.7), rather than single fixed values.

Based on the above remarks and since, in our proposed work, the qMT-MAC nodes act as traffic aggregators based on the fact that the nodes provide connectivity to RUs that, in turn, serve a large set of users, we followed the well-known traffic model of aggregated ON/OFF sources with Pareto-distributed inter-frame arrival distributions [39] (as implemented in [40]) for the aggregated UL traffic sent by the MNO's RAUs towards the centralized equipment.

References

1. Cisco Annual Internet Report (2018–2023) White Paper. Available online: https://www.cisco.com/c/en/us/solutions/collateral/executive-perspectives/annual-internet-report/white-paper-c11-741490.html (accessed on 9 April 2022).
2. Rappaport, T.S.; Xing, Y.; MacCartney, G.R.; Molisch, A.F.; Mellios, E.; Zhang, J. Overview of Millimeter Wave Communications for Fifth-Generation (5G) Wireless Networks—With a Focus on Propagation Models. *IEEE Trans. Antennas Propag.* **2017**, *65*, 6213–6230. [CrossRef]
3. Yaghoubi, F.; Mahloo, M.; Wosinska, L.; Monti, P.; de Souza Farias, F.; Costa, W.A.J.C.; Chen, J. A techno-economic framework for 5G transport networks. *IEEE Wirel. Commun.* **2018**, *25*, 56–63. [CrossRef]
4. Fallgren, M.; Timus, B. Deliverable D1.1 Scenarios Requirements and KPIs for 5G Mobile and Wireless System; 7th Framework Programme, Project METIS; 2013. Available online: https://cordis.europa.eu/docs/projects/cnect/9/317669/080/deliverables/001-METISD11v1pdf.pdf (accessed on 25 August 2022).
5. White Paper. Unified Fiber-Microwave Transport for 5G Network. Aviat and Ciena. Available online: https://aviatnetworks.com/blog/unified-fiber-microwave-transport-for-5g-networks/ (accessed on 11 August 2022).

6. *ETSI TS 138 401. 5G; NG-RAN*; Architecture Description (3GPP TS 38.401 Version 16.3.0 Release 16). Available online: https://www.etsi.org/deliver/etsi_ts/138400_138499/138401/16.03.00_60/ts_138401v160300p.pdf (accessed on 25 August 2022).
7. Ranaweera, C.; Wong, E.; Nirmalathas, A.; Jayasundara, C.; Lim, C. 5G C-RAN architecture: A comparison of multiple optical fronthaul networks. In Proceedings of the ONDM 2017, Budapest, Hungary, 15–18 May 2017.
8. *3GPP TR 38.801*; Study on New Radio Access Technology: Radio Access Architecture and Interfaces. Release 14. March 2017. Available online: https://portal.3gpp.org/desktopmodules/Specifications/SpecificationDetails.aspx?specificationId=3056 (accessed on 25 August 2022).
9. Exploring New Centralized RAN and Fronthaul Opportunities. Available online: https://www.ericsson.com/en/blog/2021/5/exploring-new-centralized-ran-and-fronthaul-opportunities (accessed on 25 August 2022).
10. Fan, Y.; Li, J.; Xu, K.; Gomes, N.J.; Lu, X.; Dai, Y.; Yin, F. Improved IEEE 802.11 point coordination function considering fiber-delay difference in distributed antenna systems. In Proceedings of the 2014 IEEE International Conference on Communications Workshops (ICC), Sydney, NSW, Australia, 10–14 June 2014; pp. 407–411.
11. Rommel, S.; Dodane, D.; Grivas, E.; Cimoli, B.; Bourderionnet, J.; Feugnet, G.; Morales, A.; Pikasis, E.; Roeloffzen, C.; van Dijk, P.; et al. Towards a Scaleable 5G Fronthaul: Analog Radio-over-Fiber and Space Division Multiplexing. *J. Lightwave Technol.* **2020**, *38*, 5412–5422. [CrossRef]
12. Kalfas, G.; Pleros, N. An agile and medium-transparent MAC protocol for 60 GHz radio-over-fiber local access networks. *J. Lightwave Technol.* **2010**, *28*, 2315–2326. [CrossRef]
13. Kalfas, G.; Vagionas, C.; Antonopoulos, A.; Kartsakli, E.; Mesodiakaki, A.; Papaioannou, S.; Maniotis, P.; Vardakas, J.S.; Verikoukis, C.; Pleros, N. Next generation fiber-wireless fronthaul for 5G mmWave networks. *IEEE Commun. Mag.* **2019**, *57*, 138–144. [CrossRef]
14. Kalfas, G.; Pleros, N.; Tsagkaris, K.; Alonso, L.; Verikoukis, C. Saturation throughput performance analysis of a medium transparent MAC protocol for 60 GHz radio-over-fiber networks. *J. Lightwave Technol.* **2011**, *29*, 3777–3785. [CrossRef]
15. Kalfas, G.; Vardakas, J.; Alonso, L.; Verikoukis, C.; Pleros, N. Non-saturation delay analysis of medium transparent MAC protocol for 60 GHz fiber-wireless towards 5G mmWave networks. *J. Lightwave Technol.* **2017**, *35*, 3945–3955. [CrossRef]
16. Xu, Z.; Wang, H.; Ji, Y. Multichannel resource allocation mechanism for 60 GHz radio-over-fiber local access networks. *J. Opt. Commun. Netw.* **2013**, *5*, 254–260. [CrossRef]
17. Panagiotakis, A.; Nicopolitidis, P.; Papadimitriou, G.I.; Sarigiannidis, P.G. Performance increase for highly-loaded RoF access networks. *IEEE Commun. Lett.* **2015**, *19*, 1628–1631. [CrossRef]
18. Datsika, E.; Kartsakli, E.; Vardakas, J.S.; Antonopoulos, A.; Kalfas, G.; Maniotis, P.; Vagionas, C.; Pleros, N.; Verikoukis, C. QoS-Aware Resource Management for Converged Fiber Wireless 5G Fronthaul Networks. In Proceedings of the 2018 IEEE Global Communications Conference (GLOBECOM), Abu Dhabi, United Arab Emirates, 9–13 December 2018; pp. 1–5.
19. Kalfas, G.; Maniotis, P.; Markou, S.; Tsiokos, D.; Pleros, N.; Alonso, N.; Verikoukis, C. Client-weighted medium-transparent MAC protocol for user-centric fairness in 60 GHz radio-over-fiber WLANs. *J. Opt. Commun. Netw.* **2014**, *6*, 33–44. [CrossRef]
20. Mesodiakaki, A.; Maniotis, P.; Gatzianas, M.; Vagionas, C.; Pleros, N.; Kalfas, G. A Gated Service MAC Protocol for Sub-Ms Latency 5G Fiber-Wireless mmWave C-RANs. *IEEE Trans. Wirel. Commun.* **2021**, *20*, 2502–2515. [CrossRef]
21. Skubic, B.; Bottari, G.; Rostami, A.; Cavaliere, F.; Ohlen, P. Rethinking optical transport to pave the way for 5G and the networked society. *J. Lightwave Technol.* **2015**, *33*, 1084–1091. [CrossRef]
22. Nakamura, S.; Yanagimachi, S.; Takeshita, H.; Tajima, A.; Hino, T.; Fukuchi, K. Optical switches based on silicon photonics for ROADM application. *IEEE J. Sel. Top. Quantum Electron.* **2016**, *22*, 3600609. [CrossRef]
23. Spatharakis, C.; Tokas, K.; Patronas, I.; Bakopoulos, P.; Reisis, D.; Avramopoulos, H. NEPHELE: Vertical Integration and Real-Time Demonstration of an Optical Datacenter Network. In Proceedings of the 2018 20th International Conference on Transparent Optical Networks (ICTON), Bucharest, Romania, 1–5 July 2018; pp. 1–4. [CrossRef]
24. Larsen, L.M.P.; Checko, A.; Christiansen, H.L. A Survey of the Functional Splits Proposed for 5G Mobile Crosshaul Networks. *IEEE Commun. Surv. Tutor.* **2019**, *21*, 146–172. [CrossRef]
25. Common Public Radio Interface (CPRI) Specification V7. 2015. Available online: http://www.cpri.info/downloads/CPRI_v_7_0_2015-10-09.pdf (accessed on 1 April 2022).
26. Zeng, Y.; Liang, Y.; Zhang, R. Blindly Combined Energy Detection for Spectrum Sensing in Cognitive Radio. *IEEE Signal Process. Lett.* **2008**, *15*, 649–652. [CrossRef]
27. Sasu, S.A.; Autenrieth, A.; Zou, J.; Elbers, J.-P. Packet Delay Variation Correction for Time Sensitive Networking with Frame Preemption. In Proceedings of the 2020 European Conference on Optical Communications (ECOC), Brussels, Belgium, 6–10 December 2020; pp. 1–3. [CrossRef]
28. Zhou, Z.; Yan, Y.; Ruepp, S.; Berger, M. Analysis and implementation of packet preemption for Time Sensitive Networks. In Proceedings of the 2017 IEEE 18th International Conference on High Performance Switching and Routing (HPSR), Campinas, Brazil, 18–21 June 2017; pp. 1–6. [CrossRef]
29. *IEEE 802.1Qbu-2016*; IEEE Standard for Local and Metropolitan Area Networks—Bridges and Bridged Networks—Amendment 26: Frame Preemption. IEEE: Piscataway, NJ, USA, 2016.
30. *IEEE 802.3Qbr-2016*; IEEE Standard for Ethernet Amendment 5: Specification and Management Parameters for Interspersing Express Traffic. IEEE: Piscataway, NJ, USA, 2016.
31. Omnet++ Discreet Event Simulator. Available online: https://omnetpp.org/ (accessed on 25 August 2022).

32. Leland, W.; Taqqu, M.; Willinger, W.; Wilson, D. On the self-similar nature of Ethernet traffic. *IEEE/ACM Trans. Netw.* **1994**, *23*, 183–193.
33. Crovella, M.; Bestavros, A. Self-similarity in World Wide Web Traffic: Evidence and possible causes. *IEEE/ACM Trans. Netw.* **1997**, *5*, 835–846. [CrossRef]
34. Beran, J.; Sherman, R.; Taqqu, M.S.; Willinger, W. Long-range Dependence in Variable Bit Rate video traffic. *IEEE Trans. Commun.* **1995**, *43*, 1566–1579. [CrossRef]
35. Oliveira, C.; Kim, J.B.; Suda, T. Long-range dependence in IEEE 802.11b wireless LAN traffic: An empirical study. In Proceedings of the 2002 14th International Conference on Ion Implantation Technology Proceedings (IEEE Cat. No.02EX505), Dana Point, CA, USA, 20–21 October 2003.
36. Wang, K.; Li, X.; Ji, H.; Du, X. Optimizing the LTE discontinuous reception mechanism under self-similar traffic. *IEEE Trans. Veh. Technol.* **2015**, *64*, 5904–5918. [CrossRef]
37. Alba, A.; Kellerer, W. Large- and Small-Scale Modeling of User Traffic in 5G Networks. In Proceedings of the 2019 15th International Conference on Network and Service Management (CNSM), Halifax, NS, Canada, 21–25 October 2019.
38. Xiang, L.; Ge, X.; Zhang, K.; Liu, C. A Self-similarity Frame Traffic Model Based on the Frame Components in 802.11 Networks. In Proceedings of the 2009 International Conference on Computational Science and Engineering, Vancouver, BC, Canada, 29–31 August 2009.
39. Taqqu, M.S.; Willinger, W.; Sherman, R. Proof of a fundamental result in self-similar traffic modeling. *ACM SIGCOMM Comput. Commun. Rev.* **1997**, *27*, 5–23. [CrossRef]
40. Synthetic Self-Similar Traffic Generation. Available online: http://research.glenkramer.com/trf_research.shtml (accessed on 11 August 2022).